Study of the Reactions $\pi^+p \to K^+\Sigma^+$ and $\pi^+p \to K^+Y^{*+}(1385)$ Between 3.5 and 14 GeV/c*

A. Bashian,† G. Finocchiaro, M. L. Good, P. D. Grannis,‡ O. Guisan,§
J. Kirz,|| Y. Y. Lee, and R. Pittman
*State University of New York at Stony Brook,** Stony Brook, New York 11790*

and

G. C. Fischer††† and D. D. Reeder
*University of Wisconsin,** Madison, Wisconsin 53706*
(Received 7 July 1971)

Measurements of the differential cross section for the reactions $\pi^+p \to K^+\Sigma^+$ and $\pi^+p \to K^+Y^{*+}(1385)$ are reported at 3.5, 3.75, 4.0, 4.25, 4.5, 4.75, 5.0, 6.0, 10.0, and 14.0 GeV/c. Polarization in $\pi^+p \to K^+\Sigma^+$ is also reported at 6.0, 10.0, and 14.0 GeV/c. At small $|t|$, the cross section for $\pi^+p \to K^+\Sigma^+$ is well described by an exponential Ae^{bt} with slopes in the range $b \approx 8-10$ (GeV/c)$^{-2}$; for $|t| > 0.5$ (GeV/c)^2 this slope decreases considerably. The cross section for $\pi^+p \to K^+Y^{*+}(1385)$ is well described for $|t| > 0.2$ (GeV/c)^2 by a single exponential of slope about half that for $\pi^+p \to K^+\Sigma^+$; there is no break near $|t| = 0.5$ (GeV/c)^2. We observe a dip in this cross section near $t = 0$. The polarization in $\pi^+p \to K^+\Sigma^+$ is consistent with zero for $|t| < 0.4$ (GeV/c)^2 and becomes large and positive for larger $|t|$.

I. INTRODUCTION

The class of reactions

$$\pi N \to KY, \tag{1}$$

where $Y = \Lambda, \Sigma, Y^*(1385)$, is interesting for a variety of reasons. Taken together with

$$\bar{K}N \to \pi Y, \tag{2}$$

the description in a Regge phenomenology[1] is relatively simple. These reactions would be expected to receive dominant contributions at large energies from the exchange of $K_V = K^*(890)$ and $K_T = K^*(1420)$ poles. Since, for $Y = \Lambda, \Sigma^+$, in reactions (1) and (2) observation of the decay asymmetry allows a polarization measurement in addition to the differential cross section, there is a variety of tests which can be made for specific models. Of particular interest is the hypothesis of exchange degeneracy[2] of K_V and K_T trajectories and/or residues; in the limit of exact degeneracy, line-reversed pairs of reactions (1) and (2) should have identical cross sections and should both display zero polarization. Departures from these predictions may then be interpreted in terms of degeneracy-breaking models[3] and possible Regge-cut contributions.[4]

A second point of interest in the reactions dominated by strange meson exchanges is that they allow determination of $S = \pm 1$ meson couplings to mesons and baryons. Such information, taken together with $S = 0$ meson couplings, permit the calculation of F/D ratios for the vector- and tensor-meson couplings with baryons. At present these are poorly known; due to model uncertainties in their computation it is desirable to have measurements on as many reactions of (1) and (2) as possible.

We report here measurements of the differential cross section and polarization in the reaction

$$\pi^+p \to K^+\Sigma^+ \tag{3}$$

and differential cross section in the reaction

$$\pi^+p \to K^+Y^{*+}(1385). \tag{4}$$

We have performed these measurements at momenta 3.5, 3.75, 4.0, 4.25, 4.75, 5.0, 6.0, 10.0, and 14.0 GeV/c. The momentum-transfer range covered expands from $|t| < 0.15$ (GeV/c)^2 at the lowest momenta to $|t| < 1.0$ (GeV/c)^2 at 10 and 14 GeV/c.

II. EXPERIMENTAL METHOD

The experiment was performed at the Brookhaven AGS in an unseparated charged two-stage beam from the G-10 target. A 24-in.-long, 2-in.-diameter liquid hydrogen target was situated at the second focus. Beam particles were identified by a set of scintillators B_1, B_2, B_3, and Čerenkov counters CB_1, CB_2 shown in Fig. 1. B_2 was used in anticoincidence to eliminate the rather large flux of muons and other particles surrounding the beam. B_3 defined the incident beam position at the target within a 1.25-in.-diameter circle. CB_1 was a threshold gas Čerenkov counter set to count π's and reject K's and p's; CB_2 was a differential gas Čerenkov counter which could be adjusted to count either K's or π's. Rejection of K^+ and p in the beam was good (>96%) as indicated by the small number of events which reconstruct as K^+p or pp elastic

scattering.

The method of detecting reactions (3) and (4) involves a single-arm magnetic spectrometer in which the forward K^+ momentum and angle are measured. There were, in addition, various counters surrounding the target to detect the decay products from Σ^+ or $Y^{*+}(1385)$. The K^+ is counted in scintillators F_1, F_2, F_3, and F_4 shown in Fig. 1. Identification of the forward particle is made with the Čerenkov counters CF_1, CF_2, and CF_3; CF_1 was a 26-in.-long, 5-in.-diameter threshold counter set to count both K and π. CF_2 and CF_3 were set to count only π. Good identification of the K^+ was necessary, since kinematically reaction (3) is almost identical to $\pi^+ p \to \pi^+ \Delta^+$ for which the cross section[5] is four times larger than it is for (3). Measurements of the efficiencies of the spectrometer Čerenkov counters indicate the probability for a π^+ recording as a K^+ is less than 0.02%. Four magnetostrictive wire spark chambers (W_1–W_4) before the spectrometer magnet and four (W_5–W_8) after the magnet measured the trajectories before and after bending to give angles of scattering and momentum. Alternate planes were rotated by 45° to remove multispark ambiguities.

For beam momenta between 3.5 and 6 GeV/c the spectrometer magnetic field was varied so as to give a fixed 10° angle of bend for the beam; at 6 GeV/c and above, the magnet was at maximum current. Up to 6 GeV/c, the momentum resolution of the spectrometer was about 45 MeV/c, nearly independent of beam momentum and limited by multiple Coulomb scattering. At 10 and 14 GeV/c, the resolutions were 66 and 102 MeV/c. Spectrometer solid-angle acceptance was 2×10^{-3} sr in the laboratory.

A view of the counters surrounding the hydrogen target is shown in Fig. 2. S_1–S_4 surround the sides of the target; at least one of these is required in the trigger to ensure a recoil particle or decay product from the target. S_5, S_6, CS_1, S_7 form the Σ^+ polarization detector; S_5 and S_6 measure, respectively, protons from $\Sigma^+ \to p\pi^0$ above and below the mean plane of scattering. CS_1 is a glycerol Čerenkov counter which detects π^+ from $\Sigma^+ \to n\pi^+$; S_7 requires that the Σ decay product traverse the polarization telescope. Counters A_1–A_4 just after the target reject events in which there were particles produced in the forward direction outside the spectrometer acceptance and guard against triggers from scatterings in CF_1. A_5 (Fig. 1) rejects events in which there was a beam particle in close time proximity to the scattering or fast forward particles in the lab.

The experimental trigger consisted of a coincidence between the beam $(B_1 \cdot \overline{B_2} \cdot B_3 = B)$, spectrometer $[F_1 \cdot F_2 \cdot F_3 \cdot F_4 \cdot \overline{(A_1+A_2+A_3+A_4+A_5)} = F]$, and recoil counters $(S_1+S_2+S_3+S_4 = S)$. Choice of particle in the spectrometer was made with the Čerenkov counters:

$$\pi = CF_1 \cdot CF_2 \cdot CF_3,$$
$$K = CF_1 \cdot \overline{(CF_2+CF_3)},$$
$$p = \overline{(CF_1+CF_2+CF_3)}.$$

Due to the large elastic-scattering trigger rate, we have triggered separately on events tagged as π incident-π scattered and on π incident-K or p scattered. Data on the reaction $\pi^+ p \to p\pi^+$ from the π-incident-p-scattered trigger will be reported elsewhere. The experiment was run with incident pion flux in the range $(1-5)\times10^5$ per burst. Trigger rates were typically 3–6 per burst for the combined class of triggers.

On receipt of a valid trigger, spark-chamber coordinates, tags of various counters, and the incident π flux since the last trigger were read into a PDP-8 computer. On-line checks were performed on the system performance and missing-mass plots produced, and the data were written on magnetic tape. Tags were included to indicate identity of beam and spectrometer particles, the occurence of more than one recoil counter firing (S_1–S_4), and the presence of a count in S_5, S_6, S_7, or CS_1.

In order to collect data at various momenta and momentum transfers, the spectrometer magnet, wire chambers, and associated counters could be

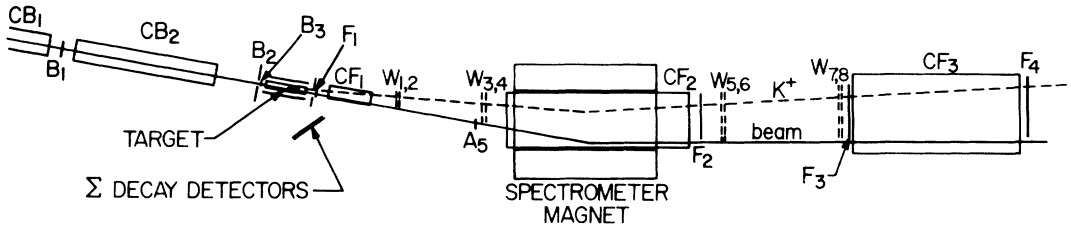

FIG. 1. Plan view of the experimental layout. W_1–W_8 are wire spark chambers; B_1–B_3, F_1–F_4, and A_5 are scintillation counters; CB_1–CB_2 and CF_1–CF_3 are Čerenkov counters. The trigger requirements are described in the text.

moved. At all momenta data were taken with spectrometer acceptance between 1° and 5° in the lab. At 6 and 10 GeV/c, data were also taken with spectrometer acceptance between $3\frac{1}{2}$° and 8°. At 6 GeV/c there was an additional run made with the spectrometer moved to accept 0° scattering. The larger angle settings involved the movement of counters A_1–A_4, F_1, and CF_1 and the addition of an additional defining counter at the exit of CF_1.

III. ANALYSIS

Events from magnetic tape were passed through a track reconstruction and fitting routine. Event candidates were subjected to the requirements that tracks before and after the magnet intersect and the upstream track segment emanate from the target region. Cuts were imposed on the χ^2 of fitting track segments and on the number of chambers participating in determining the event. Geometric limitations were imposed on the reconstructed track at the various chamber planes and at the exit of CF_1 to ensure that edge sparking effects could not influence the data. In practice the minimum angle cut for the reactions reported here occurred at the first spark chamber ($W1$) and the maximum angle cut was imposed at the exit of CF_1.

Distributions have been plotted of the reconstructed intersection of tracks at the center of the target; these distributions provide a measure of the over-all accuracy of the survey of spectrometer relative to beam and also probe the accuracy of centering the beam on the hydrogen target. We have found shifts in these distributions of up to $\frac{3}{8}$ in. A correction was applied to the spectrometer location relative to the target to center the distribution at the beam axis for sample data at each spectrometer setting.

Events passing the various geometric cuts were analyzed for the missing mass recoiling from the fast particle in the spectrometer. An example of such a mass spectrum is shown in Fig. 3. The shape of this spectrum was fitted to a sum of Gaussians for p, Σ^+, $Y^{*+}(1385)$, $Y^{*+}(1670)$, and a smooth background.[6] The functional form of the background has been chosen to represent the nonresonant multiparticle final states above $\Lambda K^+\pi^+$ threshold; the t dependence of such background has been investigated in the control region $2.2 < \mathrm{MM}^2 < 2.5$ GeV^2 and is seen to be similar to that of the Y^* data.

The geometric acceptance of the system has been computed by Monte Carlo techniques. The observed beam profile, momentum distribution, and

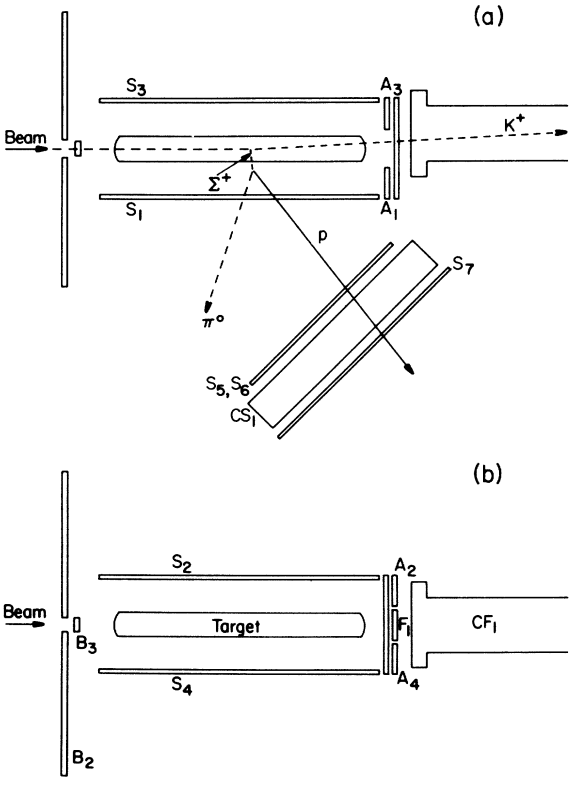

FIG. 2. Counter arrangement around the target: (a) plan view, with sketch of an event of reaction (3); (b) side view.

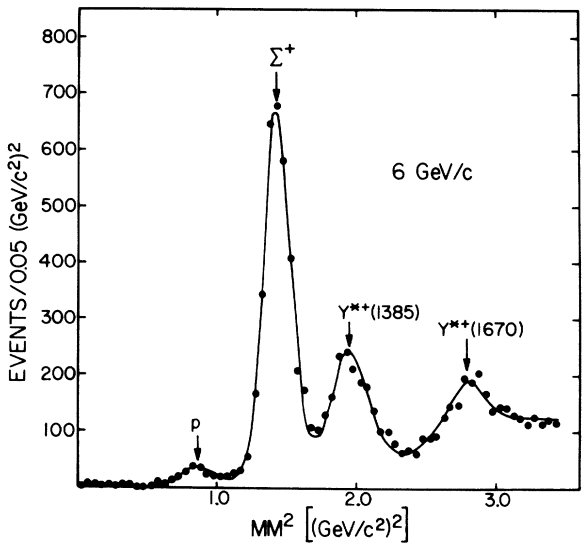

FIG. 3. Spectrum of the missing mass squared in the reaction $\pi^+ p \to K^+ X^+$ at 6 GeV/c. Contributing to the fit to the data are Gaussian distributions for the Σ^+, $Y^{*+}(1385)$ (Ref. 6) and $Y^{*+}(1670)$, a phase-space term for the $\Lambda\pi^+K^+$, $(\Sigma\pi)^+K^+$ etc. final states, and a smooth background. We have included a Gaussian for the proton to account for misidentified events near 0° in the laboratory.

measured geometry were put into these calculations. Effects of multiple Coulomb scattering, secondary nuclear scattering in CF_1 and target, and range restrictions on recoil particles have been included. In the case of the acceptance for Y^* some uncertainty (10%) arises from the lack of information on the spin alignment of the Y^*; we have used the average geometrical acceptance. The Monte Carlo calculations correctly reproduce the width of missing-mass distributions and the shape of the reconstructed intersections of tracks at the center of the target.

Corrections to the data have been made for loss of events due to K^+ decay (9–34%), K^+ interactions in the spectrometer (9–16%), and CF_1 inefficiency for K's (1–11%). Further corrections have been made for μ^+ contamination of the beam (~4%), beam attenuation in hydrogen (~4%), and the empty-target event rate (4–9%). Finally, a correction was made for failure in reconstruction due to individual spark chamber misfires or failures (<5%).

Calculation of the momentum transfer was made by a two step process: First the missing mass was computed using measured scattering angle and momentum of the K^+. If the event was within the accepted range of missing mass squared for either reaction (3) or (4), the momentum transfer was calculated using the scattering angle, and assuming that the mass of the recoiling particle was that of the Σ^+ or $Y^{*+}(1385)$.[6] This procedure gave a noticeable improvement in resolution. The t resolution varied between ± 0.005 $(\mathrm{GeV}/c)^2$ at the lowest momenta and ± 0.02 $(\mathrm{GeV}/c)^2$ at the highest momentum.

The analysis of the polarization data was made by selecting events satisfying the mass cuts appropriate to the Σ^+ from the spectrometer data and calculating the asymmetry in S_5 and S_6 counting rates

$$A = \frac{N(S_5) - N(S_6)}{N(S_5) + N(S_6)} .$$

The polarization P is given by

$$P = 2A/\alpha ,$$

where α is the decay asymmetry parameter $[\alpha(\Sigma^+ \to p\pi^0) = -0.991 \pm 0.019$ and $\alpha(\Sigma^+ \to n\pi^+) = 0.066 \pm 0.016]$ for Σ^+ decay. It was thus necessary to determine the probability for detecting the two decay modes. This was done by Monte Carlo calculations. We have found that the correction to the asymmetry due to counts from $\Sigma^+ \to n\pi^+$ varies smoothly between 10% and 25% within our range of t. The detection probability for protons from $\Sigma^+ \to p\pi^0$ is over 90% for $|t| \geq 0.5$ $(\mathrm{GeV}/c)^2$ and falls to 55% near $|t| = 0$.

In addition to the data on reactions (3) and (4) reported here, we have taken data on $\pi^+ p$ elastic scattering at all momenta. These runs provide a variety of checks of the data. Using this information we have demonstrated that the scale of missing mass is correctly calibrated. We have examined the up-down asymmetry of recoil protons from elastic scattering to verify that there are no instrumental asymmetries present and that the analysis procedure does not produce such an asymmetry. Finally it is possible to compare the elastic differential cross section determined from our data to those of previous experiments[7] throughout the range of momenta studied.

Our computation of $d\sigma/dt$ for $\pi^+ p \to \pi^+ p$ proceeds in the same manner outlined above. The sample

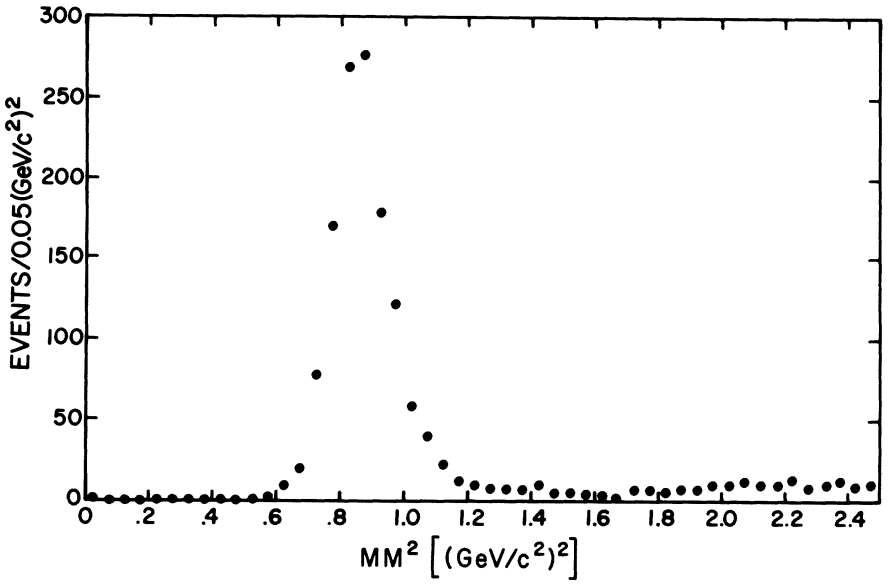

FIG. 4. Spectrum of the missing mass squared in the reaction $\pi^+ p \to \pi^+ X^+$ at 6 GeV/c.

TABLE I. Differential cross section for the reaction $\pi^+ p \to K^+\Sigma^+$. Only statistical errors are shown. Systematic errors are estimated to be ±20% and have a smooth variation with momentum transfer.

$\lvert t\rvert$ (GeV/c)^2	Momentum (GeV/c)	3.5	3.75	4.0	4.25	4.5	4.75	5.0
	$\lvert t\rvert_{\min}$ (GeV/c)^2	0.022	0.021	0.019	0.018	0.017	0.016	0.015
					$d\sigma/dt$ [μb/(GeV/c)^2]			
0.04–0.05		387 ± 29	422 ± 29	321 ± 17	329 ± 21	295 ± 19	311 ± 23	255 ± 27
0.05–0.06		424 ± 33	469 ± 33	291 ± 17	322 ± 22	284 ± 20	292 ± 21	251 ± 27
0.06–0.07		358 ± 32	411 ± 32	268 ± 18	309 ± 23	306 ± 22	307 ± 23	218 ± 27
0.07–0.08		330 ± 33	330 ± 30	247 ± 19	284 ± 24	240 ± 20	259 ± 22	250 ± 30
0.08–0.09		293 ± 35	308 ± 31	235 ± 21	238 ± 23	266 ± 23	275 ± 24	234 ± 31
0.09–0.10		282 ± 38	234 ± 29	201 ± 21	211 ± 23	287 ± 25	238 ± 24	154 ± 26
0.10–0.11		175 ± 34	256 ± 32	212 ± 25	174 ± 23	219 ± 24	222 ± 24	195 ± 31
0.11–0.12		197 ± 41	234 ± 35	201 ± 28	193 ± 25	199 ± 23	213 ± 25	165 ± 29
0.12–0.13		227 ± 64	218 ± 37	215 ± 32	133 ± 23	182 ± 24	165 ± 23	122 ± 27
0.13–0.14			187 ± 40	141 ± 30	153 ± 27	190 ± 26	185 ± 27	162 ± 33
0.14–0.15					150 ± 30	200 ± 30	113 ± 22	107 ± 29
0.15–0.16					133 ± 34	163 ± 29	149 ± 28	86 ± 27
0.16–0.17						96 ± 26	148 ± 31	124 ± 36
0.17–0.18						151 ± 34	127 ± 30	109 ± 35
0.18–0.19						121 ± 35	109 ± 32	110 ± 39
0.19–0.20							129 ± 44	

$\lvert t\rvert$ (GeV/c)^2	Momentum (GeV/c)	6	10	14
	$\lvert t\rvert_{\min}$ (GeV/c)^2	0.012	0.007	0.005
			$d\sigma/dt$ [μb/(GeV/c)^2]	
0.05–0.10		273 ± 11	132 ± 5	102 ± 4
0.10–0.15		182 ± 9	73 ± 3	59 ± 3
0.15–0.20		95 ± 4	50.3 ± 2.6	37 ± 2
0.20–0.25		60 ± 3	28.8 ± 2.0	21.1 ± 1.3
0.25–0.30		41.1 ± 2.4	19.8 ± 1.8	12.1 ± 1.0
0.30–0.35		24.9 ± 1.9	11.6 ± 1.4	7.3 ± 0.7
0.35–0.40		14.8 ± 1.4	7.0 ± 1.2	4.5 ± 0.6
0.40–0.45		10.6 ± 1.3	5.0 ± 0.9	3.7 ± 0.5
0.45–0.50		7.3 ± 1.2	3.2 ± 0.5	2.1 ± 0.4
0.50–0.55		8.3 ± 1.2	2.3 ± 0.3	1.9 ± 0.3
0.55–0.60		8.7 ± 1.3		
0.60–0.65		6.2 ± 1.2	2.0 ± 0.2	1.3 ± 0.2
0.65–0.70		7.7 ± 2.3		
0.70–0.80			1.4 ± 0.2	0.9 ± 0.2
0.80–0.90			1.4 ± 0.2	0.5 ± 0.2
0.90–1.00			1.2 ± 0.2	0.7 ± 0.2
	Parameters of the fit to $d\sigma/dt = Ae^{bt}$ for $\lvert t\rvert < 0.4$ (GeV/c)^2			
	A	564 ± 26	265 ± 12	223 ± 11
	b[a]	9.7 ± 0.5	9.7 ± 0.5	10.5 ± 0.5

[a]Systematic errors have been included in the errors given for b.

TABLE II. Differential cross section for the reaction $\pi^+p \to K^+Y^{*+}(1385)$. Only statistical errors are shown. Systematic errors are estimated to be ±25%, and have a smooth variation with momentum transfer.

$\lvert t\rvert$ (GeV/c)^2 \ Momentum (GeV/c)	3.5	3.75	4.25	4.5	4.75	5.0
$\lvert t\rvert_{min}$ (GeV/c)^2	0.047	0.043	0.036	0.034	0.032	0.030
			$d\sigma/dt$ [μb/(GeV/c)^2]			
0.04–0.06			23 ± 3	22 ± 5	18 ± 3	18 ± 5
0.06–0.08	45 ± 9	80 ± 10	44 ± 7	34 ± 6	32 ± 6	10 ± 5
0.08–0.10	77 ± 16	87 ± 13	32 ± 7	56 ± 8	46 ± 8	36 ± 11
0.10–0.12	79 ± 22	107 ± 17	48 ± 9	40 ± 8	39 ± 8	54 ± 14
0.12–0.14		80 ± 21	46 ± 10	53 ± 11	51 ± 11	54 ± 15
0.14–0.16			41 ± 17	37 ± 11	49 ± 13	22 ± 11
0.16–0.18					74 ± 19	15 ± 11
0.18–0.20						53 ± 23

$\lvert t\rvert$ (GeV/c)^2 \ Momentum (GeV/c)	6.0	10.0	14.0
$\lvert t\rvert_{min}$ (GeV/c)^2	0.024	0.014	0.009
		$d\sigma/dt$ [μb/(GeV/c)^2]	
0.04–0.06	31 ± 7	21 ± 3	18 ± 3
0.06–0.08	37 ± 7	26 ± 3	22 ± 3
0.08–0.10	27 ± 7	23 ± 2	16.5 ± 1.7
0.10–0.12	38 ± 8		
0.12–0.14	59 ± 11	20 ± 2	13.7 ± 1.4
0.14–0.16	39 ± 9		
0.16–0.20	48 ± 3	17.5 ± 1.9	14.3 ± 1.3
0.20–0.24	39 ± 3	15.0 ± 1.8	9.1 ± 1.0
0.24–0.28	31 ± 3	15.6 ± 2.0	7.8 ± 0.9
0.28–0.32	23 ± 2	11.6 ± 1.7	6.7 ± 0.9
0.32–0.36	20 ± 2	8.4 ± 1.5	3.9 ± 0.7
0.36–0.40	13.7 ± 1.8	6.5 ± 1.5	5.6 ± 0.8
0.40–0.44	12.1 ± 1.8	5.0 ± 0.9	2.3 ± 0.4
0.44–0.48	12.6 ± 1.9		
0.48–0.52	8.6 ± 1.6	2.5 ± 0.3	1.3 ± 0.3
0.52–0.56	9.0 ± 1.7		
0.56–0.64	6.4 ± 1.4	1.7 ± 0.3	1.4 ± 0.3
0.64–0.72		0.9 ± 0.2	0.6 ± 0.2
0.72–0.80		0.7 ± 0.2	0.3 ± 0.2
0.80–0.96		0.6 ± 0.1	0.3 ± 0.1

Parameters of the fit to $d\sigma/dt = Ae^{bt}$ for $0.2 < \lvert t\rvert < 0.72$ (GeV/c)^2

A	97 ± 12	70 ± 10	34 ± 5
b[a]	5.0 ± 0.5	6.2 ± 0.6	5.7 ± 0.6

[a]Systematic errors have been included in the errors given for b.

of events is quite free from background; a typical missing-mass spectrum is shown in Fig. 4. The geometric efficiency of the spectrometer varies little from that for reaction (3). The efficiency for detecting the recoil proton in counters S_1–S_4 varies rapidly for $0 \leq |t| \leq 0.04$ (GeV/c)^2 due to the stopping of the proton in the hydrogen target and tardet walls. At larger $|t|$ the recoil-proton detection efficiency becomes unity. We have not considered our elastic-scattering data in the region where the stopping correction is rapidly increasing.

Comparison of the differential cross section for $\pi^+ p \to \pi^+ p$ deduced in this experiment with previously published results[7] shows the following effects: At 6 and 10 GeV/c our results agree well in shape (t dependence) with previous data. At 14 GeV/c our results are slightly less forward-peaked than other data, while below 6 GeV/c our data show a more steeply falling cross section than other results. In all cases the absolute values of our cross sections lie about 20% below previous data.

We have performed extensive checks of various mechanisms which could be the cause of these discrepancies. The over-all normalization difference is well explained by a loss of events due to extra beam halo particles within the live time of the spark chambers. The discrepancies in the t dependence at the highest and lower momenta we have ascribed to small transverse shifts in beam position at the target. The way in which this changes the acceptance of the spectrometer can be understood as follows: For fixed small laboratory angle scattering, the cut on track position at chamber $W1$ requires that the scattering take place in the upstream portion of the target. For fixed large-angle scattering, the cut on track position at Čerenkov CF_1 requires that the original scatter take place in the downstream portion of the target. Thus the specific portion of the target and the effective length of hydrogen varies with scattering angle. The actual length of target used at any given angle varies considerably as the beam central position is moved transversely.

Monte Carlo studies have shown that beam shifts of less than $\frac{3}{8}$ in. will produce the effects seen in the data. Limited data from a hodoscope[8] just ahead of the target demonstrate that shifts approaching this magnitude were present. Analysis of the beam optics and magnet sensitivities shows that such shifts are easily possible.

Rather than attempt to adjust the beam-position parameters to achieve agreement of our $\pi^+ p$ elastic cross sections with previous data, we have renormalized our data by the ratio of previous data to our results. This gives a correction function at each momentum of the form Ce^{dt} which is then applied to data from reactions (3) and (4). We have made Monte Carlo calculations to see whether the proposed mechanism for our discrepancies does indeed produce the same correction for both elastic scattering and associated production. We find that the correction functions in the two cases are the same within less than 20%.

IV. EXPERIMENTAL RESULTS AND DISCUSSION

Our results for the differential cross section in reactions (3) and (4) are presented in Tables I and II. The errors given are statistical only and do not reflect the systematic errors arising from background subtraction and the normalization procedure. These systematic errors are estimated to be ±20% for reaction (3), ±25% for reaction (4), and are due mainly to the normalization. These estimates include errors in fitting our uncorrected $\pi^+ p$ elastic cross section data and the possible differences in running conditions and spectrometer efficiencies between $\pi^+ p \to \pi^+ p$ and reactions (3) and (4). Plots of differential cross section are shown in Figs. 5 and 6.

Results for the polarization in reaction (3) at 6, 10, and 14 GeV/c are given in Table III and shown in Fig. 7. Data below 6 GeV/c are restricted to $|t| < 0.2$ (GeV/c)^2 and show no significant polarization. Our sign convention is in agreement with standard usage, and is defined as follows: We define the normal to the production plane by $\vec{n} = \overrightarrow{\text{beam}} \times \vec{K}^+$. Then a Σ^+ with positive polarization decays preferentially with its decay proton directed oppositely to $\vec{n}$.

We call attention to the following qualitative aspects of the data: The cross section for reaction (3) is well characterized by a single exponential function for $|t| < 0.4$ (GeV/c)^2 at each momentum studied. At 6, 10, and 14 GeV/c where larger $|t|$ data exist we observe that the cross section flattens out for $|t| > 0.4$ (GeV/c)^2. This behavior is consistent with the observations of previous experiments[9-12] in the same reaction between 3 and 7 GeV/c; however, the flattening appears to be less pronounced at high momenta. These effects are similar to those observed in $\pi^- p \to K^0 \Lambda/\Sigma^0$.[13,14] No evidence for a dip near $t = 0$ is observed; this indicates the presence of a strong spin-nonflip amplitude for reaction (3). We see no evidence for formation of N^* in the direct channel; if such effects were dominant we would expect variation from smooth behavior of the differential cross section in the vicinity of 3.85 GeV/c [$\Delta(2850)$] or 5.08 GeV/c [$\Delta(3230)$].

The cross section for reaction (4) is seen to be qualitatively different from that for reaction (3).

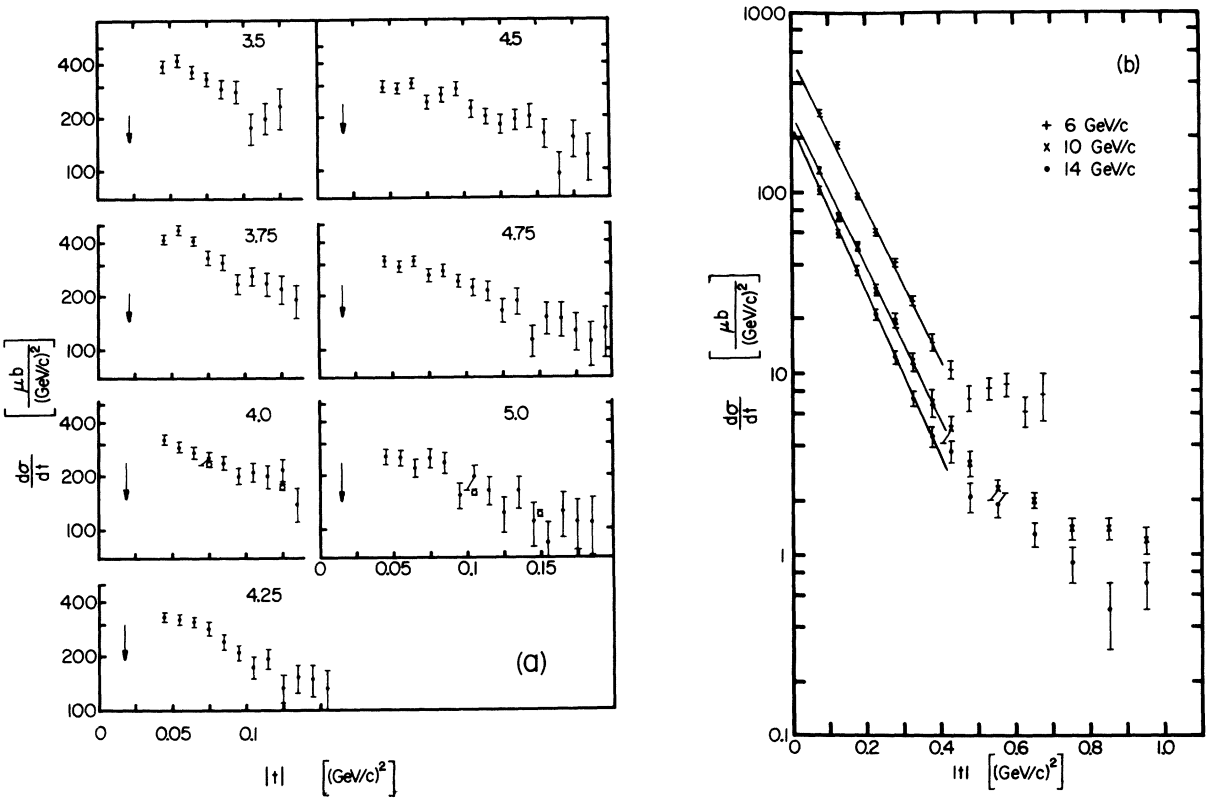

FIG. 5. Differential cross section for the reaction $\pi^+p \to K^+\Sigma^+$. (a) 3.5–5 GeV/c. Arrows indicate the kinematic limit. Open circles represent data from Ref. 10 at 4 and 5.05 GeV/c. (b) 6, 10, and 14 GeV/c. The lines represent least-squares fits to the data in the diffraction peak (see Table I).

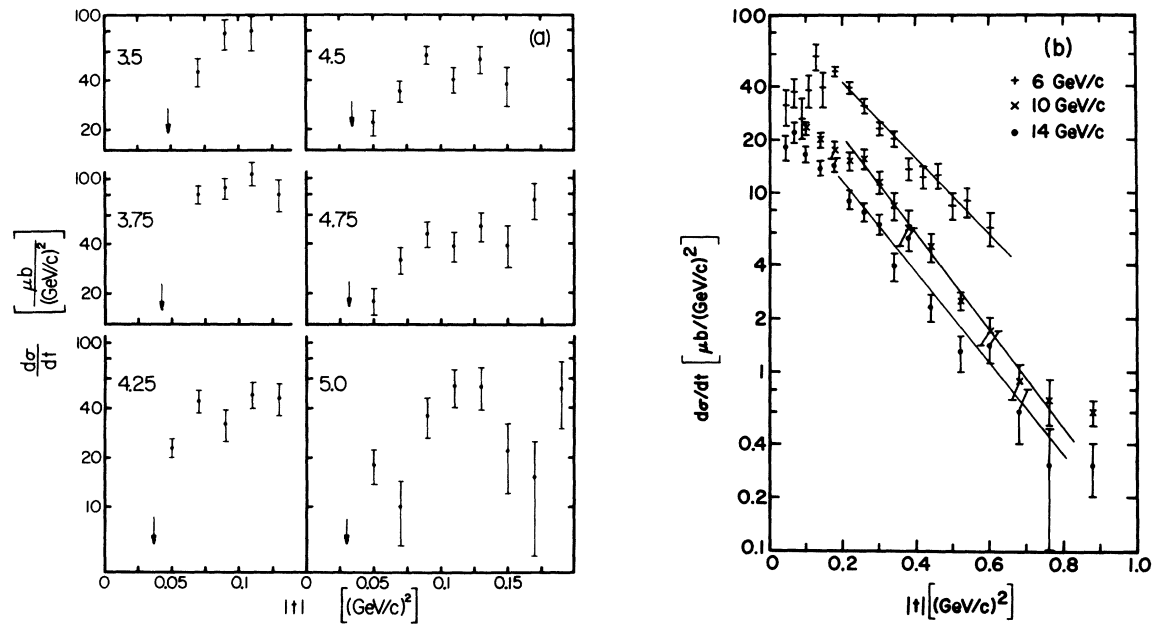

FIG. 6. Differential cross section for the reaction $\pi^+p \to K^+Y^{*+}(1385)$. (a) 3.5–5 GeV/$c$. Arrows indicate the kinematic limit. (b) 6, 10, and 14 GeV/c. The lines represent least-squares fits to the data in the range $0.2 \le |t| \le 0.72$ (GeV/c)^2. Two data points at 10 GeV/c, small $|t|$ are left off for clarity.

There is no evidence for a deviation from simple exponential behavior around $0.4 \leq |t| \leq 0.5$ (GeV/c)^2. The slope is about half that for reaction (3). These results are in agreement with previous experiments[15,16] on this reaction. Further, we see evidence that the cross section near $t = 0$ has a dip which becomes less pronounced at higher momenta.

The polarization in reaction (3) is consistent with zero at small $|t|$ with a rapid rise to large positive values for $|t| > 0.4$ (GeV/c)^2. This behavior agrees in sign and shape with that observed at lower momenta.[10]

We have fitted the forward peak in the differential cross sections for (3) and (4) with an exponential of the form $d\sigma/dt = A e^{bt}$. The results are given in Tables I and II. The range of t over which the fit was made is indicated in the table. It has been chosen to exclude the data of reaction (3) with $|t| > 0.4$ (GeV/c)^2 where the slope decreases. In reaction (4) we have excluded the forward region where the cross section exhibits a dip. We also give values for the total peripheral cross section, σ^*.[17] In Figs. 8 and 9 we show the dependence of the slope and σ^* as a function of beam momentum for our data and related hypercharge-exchange reactions.

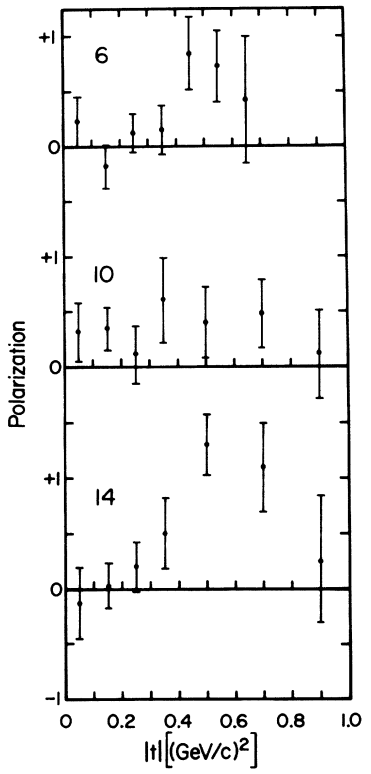

FIG. 7. Polarization of the Σ^+ in the reaction $\pi^+ p \to K^+\Sigma^+$ at 6, 10, and 14 GeV/c.

Several interesting comparisons can be made between cross sections for reactions (3) and (4). The differences in shape between these two is qualitatively similar to the comparisons in $\pi p \to \pi X$ and $pp \to pX$. As the mass of X increases, the slope of the differential cross section decreases.[18] The flattening or dip near $t = 0$ for reaction (4) also has some precedent. The reaction $\pi N \to \pi\Delta$ has a similar dip[19] which has been explained in terms of the "ρ-photon" analogy[20] applied to the coupling of the exchanged ρ to $\bar{N}\Delta$. Extension of this argument[21] to its strange-particle analog coupling $K^*\bar{N}Y^*(1385)$ then suggests the mechanism for the forward dip.

Within the context of Regge-pole models, further comparison can be made. If one assumes both reactions are dominated by K_V and K_T exchanges and that these two trajectories are approximately coincident, then the cross section can be expressed as

$$\left(\frac{d\sigma}{dt}\right)_j = f_j(t) s^{2\alpha_{\mathrm{eff}}(t)-2}. \tag{5}$$

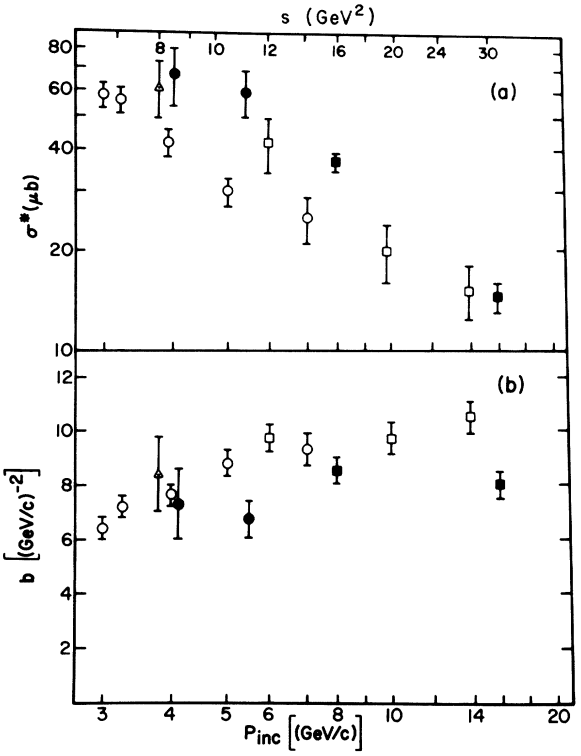

FIG. 8. Comparison of the fits to the momentum-transfer distribution for the line-reversed reactions $\pi^+ p \to K^+\Sigma^+$ and $K^- p \to \pi^-\Sigma^+$ as a function of the beam momentum. (a) The cross section $\sigma^* = \int_{-0.4}^{-0.03} A e^{bt}\, dt$. (b) The slope b. Open symbols refer to the reaction $\pi^+ p \to K^+\Sigma^+$, closed symbols to $K^- p \to \pi^-\Sigma^+$. The data are taken from Ref. 25 (■), Ref. 24 (●), Ref. 9 (△), Ref. 10 (○), and this experiment (□).

Here j labels the reaction and α_{eff} is the effective trajectory function for the combined K_V and K_T poles. There is of course no reason that the t-dependent function $f_j(t)$ should be the same for reactions (3) and (4) since the particular couplings involved are in general quite different. However, the effective trajectories obtained should be similar for the two reactions. We have computed α_{eff} for both reactions and plotted the trajectories in Figs. 10 and 11. Data from several experiments[22] were used and the results are rather sensitive to their relative normalization. For $\pi^+p \to K^+\Sigma^+$, we find from the combined data $\alpha_{\text{eff}} = 0.67 + 1.40t$, whereas from this experiment alone, we find $\alpha_{\text{eff}} = 0.56 + 0.92t$. For $\pi^+p \to K^+Y^{*+}(1385)$ the combined data yield $\alpha_{\text{eff}} = 0.60 + 1.23t$ and this experiment alone gives $\alpha_{\text{eff}} = 0.54 + 1.19t$. The errors in trajectory parameters are illustrated by the differences in fits using our data alone or combined data. We conclude that the data are in agreement with the assumption of approximately coincident K_V and K_T trajectories. The trajectory slopes obtained using this experiment alone have a value similar to those for the ρ and A_2 trajectories found from $\pi^-p \to \pi^0 n$ and $\pi^-p \to \eta n$.[23] The extrapolations of α_{eff} to positive t pass somewhat above both $K^*(890)$ and $K^*(1420)$ poles. Taken over the entire t region, the effective trajectory indicates a rather standard Regge-pole shrinkage behavior; however, the fitted slopes in the forward exponential region for reaction (3) (Fig. 8) allow considerable latitude in the range of shrinkage due to the errors. As a guide to the character of the shrinkage of the cross section and an indication of which experiments contribute to trajectory fits in different s and t regions, we show in Fig. 12 sample plots of $d\sigma/dt$ for fixed t as a function of s.

The trajectory $\alpha_{\text{eff}}(t)$ passes through zero near $t = -0.5$ (GeV/c)^2 just in the vicinity of the break in the cross section for reaction (3).

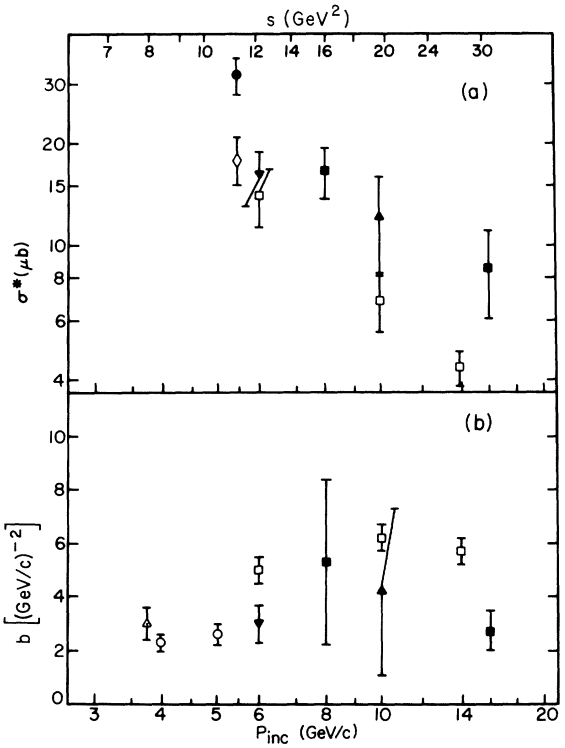

FIG. 9. Comparison of the reactions $\pi^+p \to K^+Y^{*+}(1385)$ and $K^-p \to \pi^-Y^{*+}(1385)$ as a function of the beam momentum: (a) the total peripheral cross section σ^*; (b) slope of the momentum-transfer distribution excluding the forward dip. Open symbols refer to the reaction $\pi^+p \to K^+Y^{*+}$. Closed symbols to $K^-p \to \pi^-Y^{*+}$. The data are taken from Ref. 25 (■), Ref. 28 (▼), Ref. 29 (▲), Ref. 27 (●), Ref. 11 (◇), Ref. 9 (△), Ref. 15 (○), and this experiment (□).

In order to compare the present data with predictions based on the possible exchange degeneracy of K_V and K_T poles we consider the reactions

$$K^-p \to \pi^-\Sigma^+ \qquad (6)$$

TABLE III. Σ^+ polarization in the reaction $\pi^+p \to K^+\Sigma^+$.

$\lvert t\rvert$ (GeV/c)^2 \ Momentum (GeV/c)	6	10	14
		Polarization	
<0.1	0.23 ± 0.23	0.33 ± 0.27	−0.13 ± 0.32
0.1–0.2	−0.18 ± 0.19	0.35 ± 0.19	0.03 ± 0.20
0.2–0.3	0.12 ± 0.17	0.12 ± 0.26	0.20 ± 0.23
0.3–0.4	0.15 ± 0.23	0.61 ± 0.38	0.50 ± 0.32
0.4–0.5	0.84 ± 0.33	0.40 ± 0.32	1.30 ± 0.28
0.5–0.6	0.73 ± 0.33		
0.6–0.7	0.42 ± 0.57	0.48 ± 0.31	1.11 ± 0.41
0.7–0.8			
0.8–1.0		0.12 ± 0.40	0.25 ± 0.59

and

$$K^- p \to \pi^- Y^{*+}(1385), \qquad (7)$$

which have been investigated in other experiments,[24-29] and which are, respectively, the line reversed reactions to (3) and (4). In the limit of strong exchange degeneracy (identical trajectories and equal residues for K_V and K_T), the line-reversed pairs of reactions should have equal cross sections[30] and zero polarizations. Figures 8 and 9 show the comparison for the slopes of the forward cross sections and σ^*.[17] We see that for both pairs of reactions, the π^+ induced reaction tends to have larger slope and smaller cross section than does the K^- induced reaction. The relative normalization errors between the separate experiments tend to weaken this conclusion. Polarization measurements exist only for the reaction $\pi^+ p \to K^+\Sigma^+$, but they clearly show nonzero values.[31] This observation also indicates a breaking of strong exchange degeneracy although it is difficult to assess this quantitatively since the polarization, being an interference between flip and nonflip amplitudes, is particularly sensitive to small departures from exchange degeneracy.

Based on the indication that the K^- induced cross sections are larger than the π^+ induced cross sections, we may investigate the possible sources of degeneracy breaking.[32] The simplest such model is weak exchange degeneracy[33] in which the trajectories of K_V and K_T are identical but residues un-

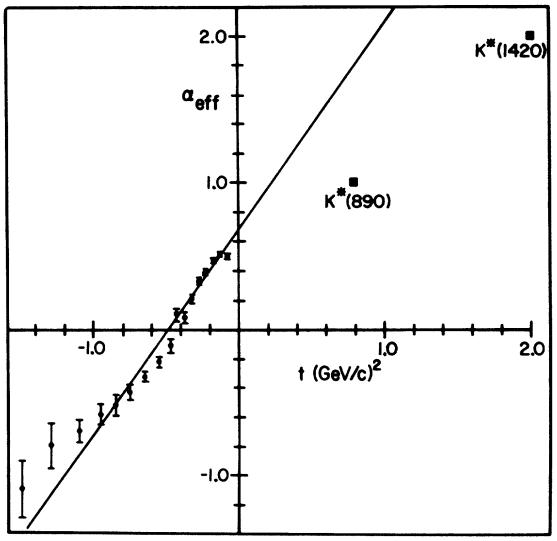

FIG. 10. Effective trajectory, $\alpha_{eff}(t)$, for the reaction $\pi^+ p \to K^+\Sigma^+$. Data points shown are fits to cross-section measurements of this experiment and Refs. 10 and 12. The line is the fit obtained for a linear trajectory.

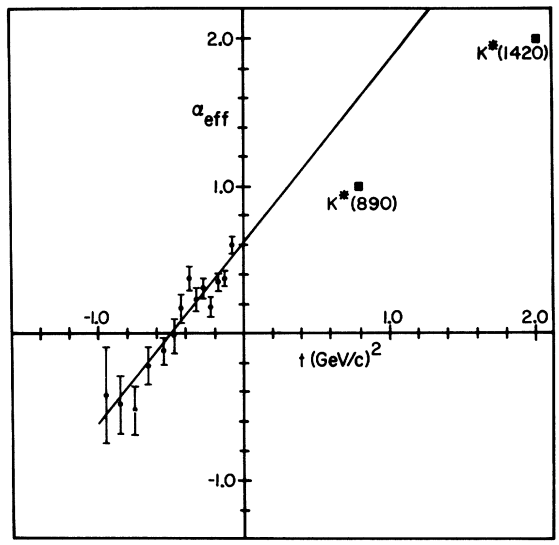

FIG. 11. Effective trajectory, $\alpha_{eff}(t)$, for the reaction $\pi^+ p \to K^+ Y^{*+}(1385)$. Data points shown are fits to cross-section measurements of this experiment, Ref. 15 and Ref. 16, Aderholz *et al*. The line is the fit obtained for a linear trajectory.

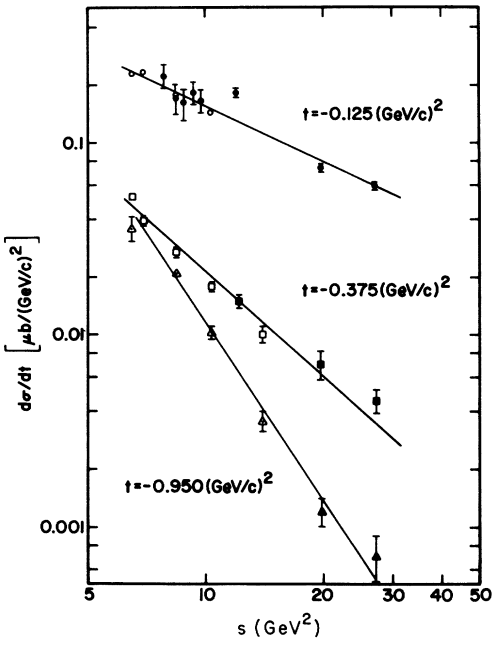

FIG. 12. Differential cross section at fixed $|t|$ for the reaction $\pi^+ p \to K^+\Sigma^+$ versus s. Sample data at $t=-0.125$, $t=-0.375$, $t=-0.950$ (GeV/c)^2 are shown. Data from this experiment are represented by closed symbols; data from Ref. 10 by open symbols. The lines represent fits to the data.

equal. Such a model allows nonzero polarization but retains the line-reversed cross-section equality and is thus inconsistent with our observations. To overcome this difficulty models have been proposed[34] in which residues are degenerate and trajectories nondegenerate and which therefore allow inequality in line-reversed cross sections. If $\alpha_V > \alpha_T$ in the forward direction one expects $\sigma(\pi^+ p \to K^+\Sigma^+) < \sigma(K^- p \to \pi^-\Sigma^+)$. However, within the framework of duality, the hypothesis of residue degeneracy without trajectory degeneracy seems unjustified.

One may examine the consequences of models in which the Regge poles are exchange-degenerate but which include Regge cuts. Here the predictions are less specific but in general all calculations agree that cross-section inequalities should exist and nonzero polarization should be expected. Sample calculations[35] involving cuts generated by Pomeranchukon and Regge poles indicate a difference between reactions (3) and (6) or (4) and (7) which is opposite to the observed effects. Calculations[36] involving cuts generated by exchange of two Regge poles give the correct sign for the cross-section difference. Finally, within the framework of the strong-cut-absorption model[37] in which pole degeneracy is not imposed it is possible to reproduce all of the features of the hypercharge exchange reactions, but with the expense of a rather large number of parameters. The physical explanation in this model for the sign of the cross-section difference is that there is a stronger absorption (larger total cross sections) in the $\pi^+ p$ channel than in the $K^- p$ channel.

Added note. After completion of this work we received a preprint by the Michigan group[38] and one by the Michigan-Argonne collaboration[39] in which further data are presented on reaction (3) at 3, 5, and 7 GeV/c and on reaction (4) at 5 GeV/c.

ACKNOWLEDGMENTS

It is a pleasure to thank Dr. Eytan Barouch, Thomas Cravens, Charles Starke, and Francois Vannuci for their contributions during the running of the experiment, and Professor Boris Kayser and Professor Chris Quigg for helpful discussions. We are grateful to Professor R. Edelstein, Dr. T. Kycia, and Professor J. Orear for the loan of their Čerenkov counters. The experiment would not have been possible without the help of the AGS staff and in particular Joseph Lypecky, the advice of J. Fuhrman, and the tireless efforts of John Moeser. Finally we acknowledge the help and service provided by the Stony Brook Computing Center.

---

*Supported in part by the U. S. Atomic Energy Commission.

†Present address: Elm Court, North Easton, Mass.

‡Alfred P. Sloan Foundation Fellow 1968–1970.

§Visitor from Centre D'Etudes Nucléaires de Saclay, Saclay, France.

||Alfred P. Sloan Foundation Fellow 1970–1972.

**During the experiment the authors held guest appointments at Brookhaven National Laboratory.

††Based in part on a thesis submitted by G. C. Fischer to the Graduate School of the University of Wisconsin in partial fulfillment of the requirements of the Ph.D. degree.

[1]D. D. Reeder and K. V. L. Sarma, Phys. Rev. 172, 1566 (1968); R. C. Arnold, *ibid.* 153, 1506 (1967); M. G. Schmidt, Nucl. Phys. B15, 157 (1970); and G. H. Renninger and K. V. L. Sarma, Phys. Rev. D 2, 1281 (1970).

[2]R. Dolen, D. Horn, and C. Schmid, Phys. Rev. 166, 1768 (1968); G. F. Chew and A. Pignotti, Phys. Letters 20, 1078 (1968).

[3]Examples of degeneracy-breaking models and further references can be found in: F. J. Gilman, Phys. Letters 29B, 673 (1969); B. R. Desai, P. Kaus, R. Park, and F. Zachariasen, Phys. Rev. Letters 25, 1389 (1970); P. R. Auvil, F. Halzen, C. Michael, and J. Weyers, Phys. Letters 31B, 303 (1970).

[4]C. Michael, Nucl. Phys. B13, 644 (1969); C. Quigg, Lawrence Radiation Laboratory Report No. UCRL 20032, 1970 (unpublished).

[5]M. Deutschmann *et al.*, Aachen-Berlin-CERN Collaboration, Phys. Letters 19, 608 (1965).

[6]We neglect the intrinsic width of the $Y^*(1385)$ because the apparent mass width in this experiment is dominated by measurement errors, particularly the uncertainty in beam momentum.

[7]C. T. Coffin, N. Dikmen, L. Ettlinger, D. Meyer, A. Saulys, K. Terwilliger, and D. Williams, Phys. Rev. Letters 17, 458 (1966); K. J. Foley, S. J. Lindenbaum, W. A. Love, S. Ozaki, J. J. Russell, and L. C. L. Yuan, *ibid.* 10, 543 (1963).

[8]A 15-element hodoscope with $\frac{1}{16}$-in. bins was present just upstream from the beam counter B_3. The inefficiency of these counters precluded direct measurement of beam-transverse profiles; they did allow however for measuring the relative shifts of the beam position at different running conditions.

[9]W. R. Butler, Lawrence Radiation Laboratory Report No. UCRL 19845, 1970 (unpublished).

[10]S. M. Pruss, C. W. Akerlof, D. I. Meyer, S. P. Ying, J. Lales, R. A. Lundy, D. R. Rust, C. E. W. Ward, and D. D. Yovanovitch, Phys. Rev. Letters 23, 189 (1969).

[11]W. A. Cooper, W. Manner, B. Musgrave, and

L. Voyvodic, Phys. Rev. Letters 20, 472 (1968). Results on $Y^*(1385)$ production from this experiment are taken from the paper by J. Mott, Nucl. Phys. B13, 565 (1969).

[12]K. S. Han, C. W. Akerlof, P. Schmueser, P. N. Kirk, D. R. Rust, C. E. W. Ward, D. D. Yovanovitch, and P. M. Pruss, Phys. Rev. Letters 24, 1353 (1970).

[13]E. Bertolucci, I. Manelli, G. Pierazzini, A. Scribano, F. Sergiampietri, M. L. Vincelli, C. Caverzasio, J. P. Guillaud, L. Holloway, and M. Yvert, Lett. Nuovo Cimento 2, 149 (1969); S. Ozaki, D. Cheng, K. J. Foley, S. J. Lindenbaum, W. A. Love, E. D. Platner, A. C. Saulys, and E. H. Willen, paper presented at the Fifteenth International Conference on High Energy Physics, Kiev, U.S.S.R., 1970 (unpublished).

[14]D. J. Crennell, G. R. Kalbfleisch, K. W. Lai, J. M. Scarr, T. G. Schumann, I. O. Skillicorn, and M. S. Webster, Phys. Rev. Letters 18, 86 (1967); M. Abramovitch, H. Blumenfeld, V. Chaloupka, S. U. Chung, J. Diaz, L. Montanet, J. Pernegr, S. Reucroft, J. Rubio, and B. Sadoulet, Nucl. Phys. B27, 477 (1971).

[15]S. P. Ying, C. W. Akerlof, D. J. Meyer, S. M. Pruss, J. Lales, R. A. Lundy, D. R. Rust, C. E. W. Ward, and D. D. Yovanovitch, Phys. Letters 30B, 289 (1969).

[16]M. Aderholz *et al.* (Aachen, Berlin, CERN, Cracow, Warsaw Collaboration), Nucl. Phys. B11, 259 (1969); D. W. Davies, M. A. Abolins, O. I. Dahl, J. S. Danburg, P. Hoch, J. Kirz, D. H. Miller, and R. K. Rader, Phys. Rev. D 2, 506 (1970).

[17]We define σ^* for the reactions $\pi^+ p \to K^+ \Sigma^+$ and $K^- p \to \pi^- \Sigma^+$ by

$$\sigma^* = \int_{-0.4}^{-0.03} A e^{bt} dt ,$$

where A and b are parameters of the fit to the forward differential cross section. For reactions $\pi^+ p \to K^+ Y^{*+}(1385)$ and $K^- p \to \pi^- Y^{*+}(1385)$ we take

$$\sigma^* = \sum_i \left(\frac{d\sigma}{dt}\right)_i \Delta t_i ,$$

where $(d\sigma/dt)_i$ is the measured differential cross section and the sum extends over $t_{\min} < |t| \leq 0.64$ (GeV/c)^2. Where this is unavailable, total measured peripheral cross sections are plotted on Fig. 9.

[18]See G. Bellettini, in *Proceedings of the Fourteenth International Conference on High Energy Physics, Vienna, 1968*, edited by J. Prentki and J. Steinberger (CERN, Geneva, Switzerland, 1968).

[19]See, for example, Aachen-Berlin-Birmingham-Bonn-Hamburg-London (Imperial College)-München Collaboration, Phys. Letters 10, 229 (1964).

[20]L. Stodolsky and J. J. Sakurai, Phys. Rev. Letters 11, 90 (1963).

[21]For recent versions of this model, for a summary of the experimental evidence, and for references to earlier work see G. H. Renninger and K. V. Sarma, Phys. Rev. 178, 2201 (1969); see also K. Kajantie and P. V. Ruuskanen, Nucl. Phys. B13, 437 (1969).

[22]In addition to the data of the present experiment we use those of Refs. 10, 12, and 15 and Ref. 16, Aderholz *et al.*

[23]Typical values for the ρ trajectory are $\alpha_\rho = 0.58 + 1.05t$, and for the A_2 trajectory $\alpha_{A_2} = 0.4 + 0.6t$. We quote also α_{eff} from other hypercharge exchange reactions for comparison: for $\pi^- p \to K^0 \Lambda/\Sigma^0$ (Ref. 13, Bertolucci *et al.*) $\alpha_{\text{eff}} = 0.34 + 0.15t$; our determination from data on $K^- p \to \pi^- \Sigma^+$ (Refs. 24 and 25) gives $\alpha_{\text{eff}} = 0.47 + 0.70t$; our determination for $K^- p \to \pi^- Y^{*+}(1385)$ (Refs. 25, 28, and 29) gives $\alpha_{\text{eff}} = 0.66 + 1.3t$.

[24]J. S. Loos, U. E. Kruse, and E. L. Goldwasser, Phys. Rev. 173, 1330 (1968).

[25]D. Birnbaum, R. M. Edelstein, N. C. Hien, T. J. McMahon, J. F. Mucci, J. S. Russ, E. W. Anderson, E. J. Bleser, H. R. Blieden, G. B. Collins, D. Garelick, J. Menes, and F. Turkot, Phys. Letters 31B, 484 (1970).

[26]Birmingham-Glasgow-London (Imperial College)-Oxford-Rutherford Collaboration, Phys. Rev. 152, 1148 (1966).

[27]J. Mott, R. Ammar, R. Davis, W. Kropac, D. Slate, B. Werner, S. Dagan, M. Derrick, T. Fields, J. Loken, and F. Schweingruber, Phys. Rev. 177, 1966 (1969).

[28]Birmingham-Glasgow-London (Imperial College)-München-Oxford-Rutherford Collaboration, Nuovo Cimento 53A, 522 (1968).

[29]Aachen-Berlin-CERN-London (Imperial College)-Vienna Collaboration, Nucl. Phys. B7, 111 (1968).

[30]For a discussion on exchange degeneracy, and a comparison with experimental results, see the review by K. W. Lai and J. Louie, Nucl. Phys. B19, 205 (1970); and J. Kirz, in *High Energy Collisions*, edited by C. N. Yang *et al.* (Gordon and Breach, New York, 1969).

[31]Polarization data are reported in Refs. 10 and 12 in addition to the present experiment.

[32]For a summary of patterns of exchange degeneracy breaking see C. Quigg, Ref. 4.

[33]See, for example, F. J. Gilman, Ref. 3.

[34]P. R. Auvil *et al.*, Ref. 3.

[35]C. Meyers and Ph. Salin, Nucl. Phys. B19, 237 (1970). See also Ref. 4. More recently C. Meyers *et al.* [Nucl. Phys. B23, 99 (1970)] have indicated that the correct sign of the line-reversed cross section difference can be obtained by consideration of both residue-nondegeneracy and Pomeranchuk-Regge cuts.

[36]P. J. O'Donovan, Arizona State University Report No. ASU-HEP-13, 1970 (unpublished); F. S. Henyey, G. L. Kane, and J. J. G. Scanio, Phys. Rev. Letters 27, 350 (1971).

[37]F. Henyey, G. L. Kane, J. Pumplin, and M. Ross, Phys. Rev. 182, 1579 (1969); M. Ross, F. Henyey, and G. L. Kane, Nucl. Phys. B23, 269 (1970).

[38]P. Kalbaci, C. W. Akerlof, P. K. Caldwell, C. T. Coffin, D. I. Meyer, P. Schmueser, and K. C. Stanfield, Phys. Rev. Letters 27, 74 (1971).

[39]C. W. Akerlof, P. K. Caldwell, P. Kalbaci, D. I. Meyer, K. C. Stanfield, P. N. Kirk, A. Lesnik, D. R. Rust, C. E. W. Ward, and D. D. Yovanovitch, Phys. Rev. Letters 27, 219 (1971).